



HAL
open science

Roughness Variation Impact on the Morphological Evolution at the Medjerda River: Telemac 2D-Sisyphe Modeling

Saber Hammami, Hela Romdhane, Amel Soualmia, Azeddine Kourta

► **To cite this version:**

Saber Hammami, Hela Romdhane, Amel Soualmia, Azeddine Kourta. Roughness Variation Impact on the Morphological Evolution at the Medjerda River: Telemac 2D-Sisyphe Modeling. *Environment and Natural Resources Journal*, 2025, 23 (1), pp.65-79. 10.32526/enrj/23/20240043 . hal-04942763

HAL Id: hal-04942763

<https://hal.science/hal-04942763v1>

Submitted on 17 Feb 2025

HAL is a multi-disciplinary open access archive for the deposit and dissemination of scientific research documents, whether they are published or not. The documents may come from teaching and research institutions in France or abroad, or from public or private research centers.

L'archive ouverte pluridisciplinaire **HAL**, est destinée au dépôt et à la diffusion de documents scientifiques de niveau recherche, publiés ou non, émanant des établissements d'enseignement et de recherche français ou étrangers, des laboratoires publics ou privés.



Distributed under a Creative Commons Attribution - NonCommercial 4.0 International License

Roughness Variation Impact on the Morphological Evolution at the Medjerda River: Telemac 2D-Sisyphe Modeling

Hammami Saber^{1,2}, Romdhane Hela¹, Soualmia Amel^{1*}, and Kourta Azeddine²

¹National Institute of Agronomy of Tunisia, University of Carthage, 43 Avenue Charles Nicolle, 1082 Tunis, Tunisia

²University of Orléans, INSA-CVL, PRISME, EA 4229, 45072, Orléans, France

ARTICLE INFO

Received: 20 Feb 2024

Received in revised: 4 Nov 2024

Accepted: 11 Nov 2024

Published online: 3 Jan 2024

DOI: 10.32526/ennrj/23/20240043

Keywords:

Telemac-Sisyphe Model/ Sediment transport/ Vegetation/ River stability/ Medjerda River

* Corresponding author:

E-mail: amel.inat@hotmail.fr

ABSTRACT

Sediment transport plays a vital role in river management and flood protection, particularly in regions prone to erosion and deposition. The study aims to assess the impact of roughness modification on the sediment transport process in the Medjerda, Tunisia's longest perennial river, following a decade of dredging activities implemented for flood protection measures in the Boussalem city. We used the Telemac Sisyphe model to simulate a 17.8 km section, which regularly undergoes dredging crossing the city of Boussalem. This section contains two distinct parts: first a smooth riverbed followed by the variable roughness on both sides of the banks, which is influenced by the existing vegetation cover. The study developed four simulation scenarios, with a smooth riverbed maintained in all cases while the roughness of the second part increasing from smooth to rough. The model-generated outputs facilitated a comprehensive longitudinal and transverse comparative analysis, focusing on flow velocity, shear stress, and bed evolution profile in response to varying roughness levels. The results show a reduction in erosion and deposition phenomena as the roughness of the bank's roughness increases. This is the crucial role of vegetation in stabilizing river banks by strengthening the cohesion of the riverbed, thus minimizing erosion risks and excessive sediment transport, ultimately maintaining the riverbed's integrity. These findings contribute to understanding of sedimentation patterns in the Medjerda River and facilitated the prediction of potential impacts on its fluvial morphology.

1. INTRODUCTION

Erosion processes, sediment supply, and their transport are essential elements of river system functioning (Nazi et al., 2016), significantly influencing river morphology by altering their shape and structure over time. The mechanisms of aggradation, characterized by sediment accumulation, and degradation, resulting from bed erosion, contribute to the development of a distinct topography within the riverbed (Mugade Mugade and Sapkale, 2015). These dynamic processes, which are influenced by the movement and redistribution of sediment particles (Vargas-Luna et al., 2019), play a key role in the continuous evolution of river morphology, leading to a distinct and recognizable geomorphological

configuration. However, the transport capacity of a river channel can diminish when large quantities of sediment accumulate in the riverbed, increasing the risk of the rivercourse shifting into adjacent areas (Badoux et al., 2014; Rickenmann et al., 2016). Typically, sediment transport rates are estimated using empirical equations (Meyer-Peter and Müller, 1948; van Rijn, 1984; Einstein, 1950; Wilcock and Crowe, 2003), which are largely based on laboratory experiments that often oversimplify real-world conditions. More recent equations, which incorporate some field data, offer improved accuracy in representing natural processes (Recking, 2013).

Riverbanks provide a particularly favorable environment for vegetation. This vegetation increases

local roughness, alters flow patterns, and adds additional resistance, thereby reducing bed shear stress and promoting local sediment deposition (Luca et al., 2020). Roughness increases with the height and density of the vegetation. Vegetation significantly reduces sediment transport rates, especially when vegetation density is high (Penna et al., 2022; Li et al., 2022). Fortes et al. (2022) demonstrated, using a dynamic roughness model, that the water level profile increased by an average of 7.03%, thereby inferring the seasonal effect of vegetation. Fan et al. (2023) studied the relative roughness of riverbanks compared to the bed roughness, a key factor in the anti-erosion of river boundaries, using a rectangular cross-sectional model. The results reveal an optimal width-to-depth ratio for each value of relative roughness (λ). Thus, an increase in λ leads to a 36.46% reduction in river width and a 28% increase in depth. Furthermore, Fan et al. (2020) demonstrated that varying the bank angle from 0° to 60° results in a 34.84% increase in channel width and a 13.29% decrease in depth, with other hydraulic parameters remaining relatively constant.

In recent decades, rivers worldwide have been subjected to significant anthropogenic interventions, such as bank reinforcement, dam construction, urban expansion in floodplains, agricultural development, and deforestation practices (Nanson et al., 2010). Morphological models coupled with hydrodynamic models (Reisenbüchler et al., 2019) have now been applied to various rivers of different sizes and characteristics to examine channel evolution (Guan et al., 2016; Tu et al., 2017; Ramirez et al., 2020). For example, Yassine et al. (2023) developed a 2D hydromorphodynamic model with the TELEMAC-MASCARET system for the section of Lac des Gaves in the Hautes-Pyrénées to reproduce bed changes following the 2018 flood. Their study showed that the Meyer-Peter-Müller and Recking sediment transport equations, coupled with Ferguson and Strickler friction laws, are crucial for realistic simulations. Meanwhile, Nazarjani et al. (2023) revealed significant instability in 71% of the Kashafrud River sections in Iran, with high erosion potential exacerbated by human activities such as land use changes and dredging. This instability has already led to the demolition of some infrastructure due to severe erosion, highlighting the impact of human interventions on fluvial conditions.

The Medjerda is the only perennial river in Tunisia, collecting half of the country's exploitable surface water from the north. Significant sediment

deposits, partly due to frequent moderate floods and hydraulic structures, have led to modifications in the riverbed (Gharbi, 2016). Various studies have analyzed sediment transport processes in the Medjerda, notably Gharbi et al. (2016), who used Telemac 2D and Sisyphé to study sediment transport during floods and its effects on river morphology, demonstrating a close link with flood issues. Morri et al. (2016) applied the same model to simulate flow, sediment transport, and morphological changes in the presence of vegetation, integrating hydraulic resistance through an adapted friction coefficient in the Medjerda.

In our previous work, we modeled flows in the Medjerda River using TELEMAC 2D and HEC-RAS to map floods and assess the impact of dredging works, as well as to create scenarios and risk maps for return periods up to 100 years. Our calibration results revealed the Manning's coefficient values for the different studied areas as follows: minor bed (without vegetation): 0.033 s/m^{1/3}, middle bed occupied by Tamarix: 0.10 s/m^{1/3}, cleared middle bed: s/m^{1/3}, major bed (agricultural zone): s/m^{1/3}, and major bed (urban zone): 0.2 s/m^{1/3} (Hammami et al., 2022; Hammami et al., 2023; Hammami et al., 2024). Consequently, the roughness of the riverbanks ranges between 0.03 s/m^{1/3} (smoother, dredged) and 0.10 s/m^{1/3} (rougher, dense vegetation). The objective of this study is to determine the impact of the relative roughness of the banks on the morphology of the wadi, shear stress, and consequently, on sediment transport in the river. To achieve this, the Telemac2D hydrodynamic model was coupled with the Sisyphé sediment transport model. This combination allows for detailed simulation of the complex interactions between water flow, bank roughness, and sediment transport processes, to better understand and predict morphological changes in the riverbed under different conditions. To this end, we maintained the river's minor bed smooth while progressively increasing the roughness of the banks from 0.03 s/m^{1/3} to 0.09 s/m^{1/3}. This approach allows for the analysis of the effects of increasing bank roughness on hydrodynamic and sedimentary parameters.

2. METHODOLOGY

2.1 Study area

A stretch of the Medjerda River passing through the city of Boussalem, located between the coordinates 36°36'40" N, 8°58'11" E, within the alluvial plain of the upper Medjerda Valley, has been selected to

illustrate the aforementioned impacts, where the Medjerda River undergoes regular dredging works to combat flooding. The total length of this section is 17.8 km. The study area is situated 20 km upstream from the Sidi Salem Dam (Figure 1), which has a significant influence on sedimentation in the study

section. Indeed, since its construction and impoundment, the dam has resulted in the formation of a sediment plug at the entrance of the reservoir, requiring approximately the Boussalem City to be reached for the dam's impact to dissipate.

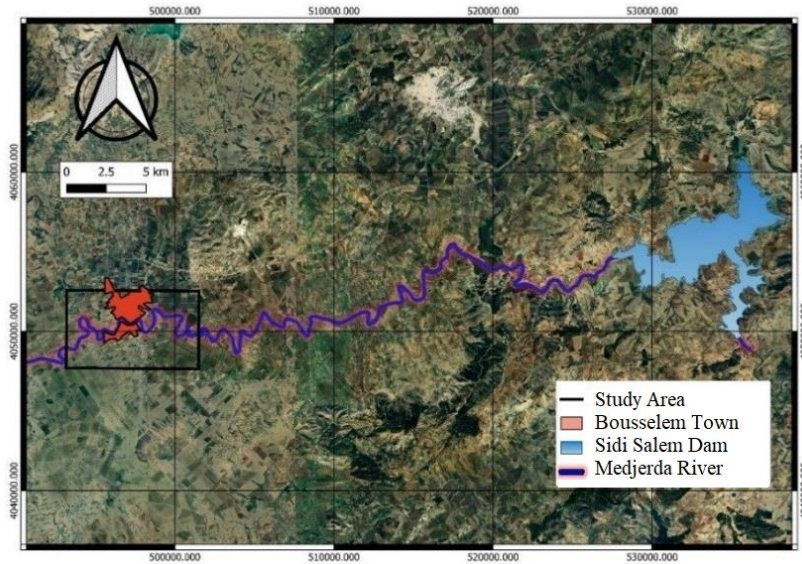


Figure 1. Location of the study area (Boussalem City: 36°36'40" N, 8°58'11" E)

2.2 Model and conceptual scheme

The TELEMAC-MASCARET system, an open-source software, is used for numerical simulations, including free surface flows, sediment transport, waves, and water quality (Hervouet, 2003). To model hydrodynamic and morphodynamic processes, we have selected the TELEMAC2D and SISYPHE modules. TELEMAC2D is used to simulate free surface flows and hydrodynamic interactions, while SISYPHE is employed to model sediment transport and morphological changes in the riverbed. The integration of these two modules allows for a comprehensive and coherent analysis of river dynamics under different roughness conditions, providing a powerful tool for studying riverbed evolution and sediment interactions.

For suspended sediment transport, SISYPHE solves the advection-diffusion equation for sediment concentration, accounting for turbulence effects and settling velocities, which is essential for simulating the movement of particles in the water column. Meanwhile, bedload transport is modeled using specific equations, such as the Meyer-Peter and Müller equation, to represent the movement of sediments along the riverbed under the influence of flow forces.

2.2.1 Hydrodynamic module

TELEMAC 2D solves the Saint-Venant equations to simulate free surface flows, which are decomposed into mass and momentum conservation equations.

$$\frac{\partial h}{\partial t} + u \times \nabla(h) + h \nabla \times (u) = 0$$

$$\frac{\partial u}{\partial t} + u \times \nabla(u) = -g d_x z f - g S_{f,x} + h^{-1} \nabla \times (h v_t \nabla u)$$

$$\frac{\partial v}{\partial t} + u \times \nabla(v) = -g d_y z f - f S_{f,y} + h^{-1} \nabla \times (h v_t \nabla v)$$

Where; t [s] is the time, $\nabla = \partial x, \partial y$ is the gradient field, $g = 9.81 \text{ ms}^{-2}$ is the acceleration due to gravity, h [m] is the water depth, $u=(u,v)$ [m/s] is the average depth velocity vector with u and v [ms^{-1}] being the components along the longitudinal x and transverse y axes, respectively, with $\{u\}$ [ms^{-1}] being the magnitude of u , and v_t [m^2s^{-1}] is the turbulent viscosity term.

2.2.2 The 2D sediment transport model

In SISYPHE, there are two sediment transport modes based on transport mechanisms: bed load and suspended load:

$$q_t = q_b + q_s$$

Where; q_t is the total sediment transport, q_b is the bed load transport, and q_s is the suspended load transport.

2.2.3 Suspended sediment transport module

Suspended transport is the portion of sediment carried by a liquid flow that settles slowly enough that it almost never touches the bed. It is kept in suspension due to the turbulence of the moving water and typically consists of fine sand particles, silt, and clay. Suspended sediment transport is accounted for by SISYPHE by solving the two-dimensional advection-diffusion equation, expressed by:

$$\frac{\partial hc}{\partial t} + \frac{\partial hu_c}{\partial x} + \frac{\partial hv_c}{\partial y} = \frac{\partial}{\partial x} \left(h \varepsilon_s \frac{\partial c}{\partial x} \right) + \frac{\partial}{\partial y} \left(h \varepsilon_s \frac{\partial c}{\partial y} \right) + E - D$$

Where; $c=c(x, y, t)$ is the depth-averaged concentration expressed as a volume percentage (-), and ε_s is the turbulent diffusivity of sediments, often related to the turbulent viscosity $\varepsilon_s = \frac{\nu_t}{\sigma_c}$, with σ_c being the Schmidt number, equal to 1.0 in SISYPHE. The non-cohesive deposition rate is $D = w_s C_{Z_{ref}}$, where w_s is the sedimentation velocity and Z_{ref} is the concentration near the bed, assessed at the interface between bed load and suspended load transport, $=Z_{ref}$. The non-cohesive erosion rate is $=w_s C_{eq}$, where C_{eq} is the equilibrium concentration near the bed determined using an empirical formula.

2.2.4 Bedload sediment transport

The term “bedload” refers to the particles in a moving fluid (typically water) that are transported along the bed. Bedload moves through rolling, sliding, and/or saltation (hopping). The morphodynamic module is based on the Exner equation (Exner, 1920), which can be coupled with the hydrodynamic module equation.

$$(1 - \gamma) \frac{\partial Z_b}{\partial t} + \nabla \times Q_b = 0$$

With Q_b being the volumetric transport rate per unit width without pores (m^2/s), Z_b the bed elevation (m), and γ the bed porosity. The dimensionless sediment transport rate induced by the current q_b^* is expressed by:

$$q_b^* = \frac{Q_b}{\sqrt{g(\rho_s - \rho)d^3}}$$

With ρ_s being the sediment density (kg/m^3); ρ the water density (kg/m^3); and d the grain diameter ($=d_{50}$ for a uniform sediment distribution (m)). Bedload transport formulas are generally calculated based on the Shields number θ , given by the formula:

$$\theta = \frac{\mu \tau_b}{(\rho_s - \rho)gd}$$

With τ_b being the bed shear stress [Pa] and μ the correction factor for surface friction. The Meyer-Peter-Müller equation is a threshold equation, and its original formulation considers a critical Shields parameter equal to 0.047. The equation is written as follows:

$$q_b^* = 8(\theta - \theta_{cr})^{3/2} = 8(\tau^* - \tau_c^*)^{3/2}$$

Where; τ^* is the critical bed shear stress, expressed as $\tau^* = \frac{\tau}{(\rho_s - \rho)d_{50}}$ and $\tau_c^* = 0.047$ is the minimum shear stress required to initiate sediment particle movement, often called the critical shear stress, which is a key parameter in sediment transport. It corresponds to the force exerted by the water flow on the sediment particles that is sufficient to overcome resisting forces, such as cohesion and weight, thereby causing the onset of particle movement.

Knowing that:

- The hydraulic friction coefficient Manning-Strickler is $= \frac{U}{R_h^{3/2} S^{1/2}}$, where U [ms^{-1}] is the average flow velocity, S [mm^{-1}] is the bed slope, and R_h [m] is the hydraulic radius.

- The grain roughness coefficient can be estimated based on the grain size distribution as $K' = \frac{26}{d_{90}^{1/6}}$, where d_{90} is the diameter corresponding to approximately 90% by weight of the grains.

The Meyer-Peter-Müller equation is written as follows:

$$q_b^* = 8 \left[\left(\frac{K'}{K} \right)^{3/2} \tau^* - 0.47 \right]^{3/2}$$

The Telemac-Sisyphe coupling is designed to address a set of morphodynamic issues (sediment transport and bed evolution) and is particularly suited for assessing sediment stock response to hydrodynamic conditions, notably bed shear stress. This coupling represents an integrated approach for the numerical modeling of free-surface flows and sediment transport in riverine, estuarine, and coastal

environments. These two models are often used synergistically to provide a more comprehensive representation of hydrodynamic and sedimentary processes.

The coupling is achieved in a chained fashion with an update of the domain geometry for each time step. In other words, the hydrodynamic module is executed first, followed by the morphodynamic module using the hydrodynamic results (Gharbi et al., 2016). Subsequently, an update of the domain geometry is performed before the next time step (Figure 2).

2.3 Roughness calibration

In our previous work, we modeled flows in the Medjerda River using TELEMAC 2D and HEC-RAS to map floods and assess the impact of dredging operations. The calibration results provide Manning’s roughness coefficient values for the different studied areas: minor bed (without vegetation): 0.033 s/m^{1/3},

middle bed occupied by Tamarix: 0.10 s/m^{1/3}, dredged middle bed: 0.4 s/m^{1/3}, major bed (agricultural area): 0.6 s/m^{1/3}, and major bed (urban area): 0.2 s/m^{1/3} (Hammami et al., 2023). Therefore, the roughness of the banks ranges from 0.03 s/m^{1/3} (smoother, dredged) to 0.10 s/m^{1/3} (rougher, dense vegetation).

We chose a simplified configuration of the river section containing two distinct parts: the first part, located at the riverbed, which is completely smooth with a roughness coefficient of 0.03 s/m^{1/3}, and includes the minor bed and the dredged middle bed. The second part, located on both sides of the banks, has variable roughness depending on the pre-existing vegetation cover (Figure 3). The scenarios we studied were designed with a fixed roughness for the riverbed, kept smooth, while the roughness of the banks was varied from the smoothest to the roughest. Four simulation scenarios were established, progressively increasing the roughness of the banks with respective values of 0.03 s/m^{1/3}, 0.05 s/m^{1/3}, 0.07 s/m^{1/3}, and 0.09 s/m^{1/3}.

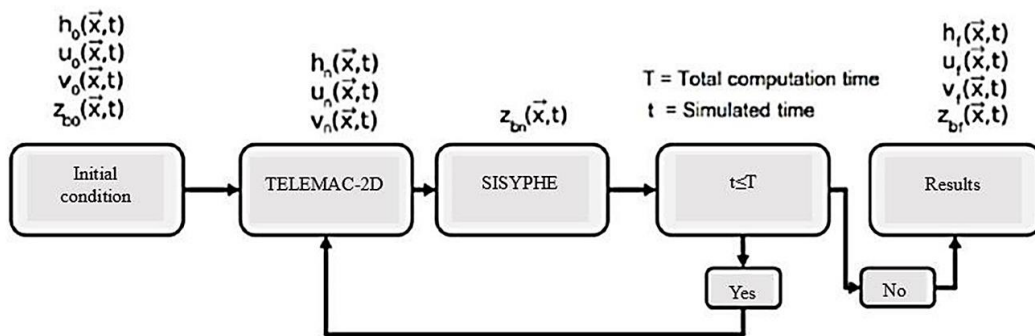


Figure 2. Simplified diagram of the Telemac-Sisyph coupling

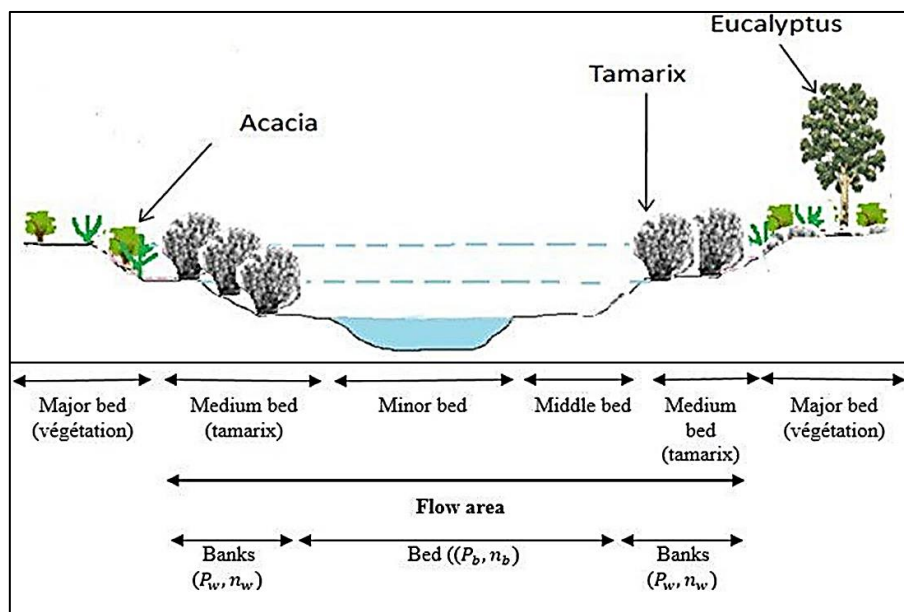


Figure 3. Roughness distribution in the Medjerda Section

To assess the impact of the non-uniform distribution of boundary roughness on the river morphology, we selected Einstein's method (Einstein, 1942; Einstein, 1950), which suggested using hydraulic radius segmentation to partition boundary resistance. This method incorporates Manning's formula for channel resistance segmentation. The specific formulation is as follows:

$$(n)^{3/2}P = (n_b)^{3/2} P_b + (n_w)^{3/2} P_w$$

Where; n_b and n_w are respectively the overall roughness coefficient of the cross-section, the roughness coefficient of the riverbed, and the roughness coefficient of the bank, and P , P_b , and P_w are respectively the wetted perimeter of the entire cross-section, the riverbed, and the bank.

$$P = P_b + P_w$$

The relative roughness of the banks compared to the riverbed is represented by the variable λ , defined as follows:

$$\lambda = (n_w)^{3/2}/(n_b)^{3/2}$$

2.4 Data and post-processing

This research requires primary data, particularly post-processing of topographic data. The considered area covers an equal surface of 40.71 km² with a river length of approximately 17.8 km. We created an unstructured surface mesh using the Blue Kenue model, based on the finite element method. This mesh was generated from a set of points derived from a LIDAR survey covering the area of interest, including riverbeds and floodplains. The LIDAR data was obtained from the Ministry of Agriculture.

Given the main objective of our study, which focuses on flows in the minor channel with relatively low discharge that does not impact floodplains, we opted for a variable mesh. More specifically, we chose a finer mesh for the minor channel, with a mesh size of approximately 5 m longitudinally to accurately represent flows along the main direction. For the rest of the domain, the mesh size is maintained at around 50 m. The grid, illustrated in the figure, consists of 54,279 nodes and 108,211 elements (Figure 4).

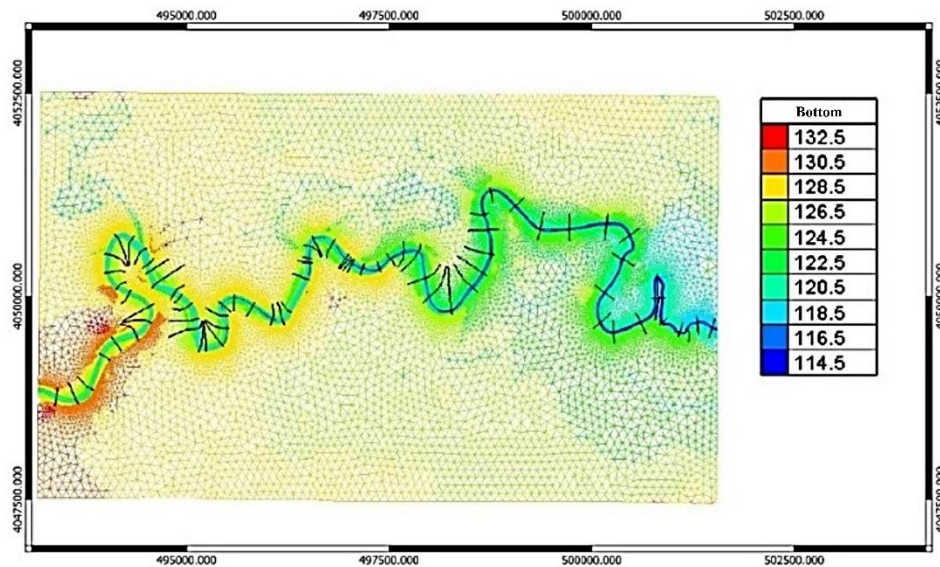


Figure 4. Study area grid with Telemac 2D

2.5 Sediment size distribution

A crucial aspect of sediment transport modeling is visualizing the evolution of sediment composition in relation to variations in flow. This visualization helps to better understand how changes in flow conditions affect the grain size distribution of sediments, their erosion, deposition, and consequently, the morphological evolution of the riverbed over time. The grain size distribution of sediments in the Oued Medjerda was

determined through sieving and sedimentation after a sampling campaign under different flow conditions. These analyses, conducted by DGRE (2004), are used in this study.

For evaluating sediment transport rates, unlike conventional models that consider only a single average diameter, SISYPHE offers a non-uniform (multi-size) model. These non-uniform sediment models rely on a complex sedimentary description,

considering several granulometric fractions that closely resemble real-world conditions.

While suspended sediment transport is predominant, the impact of bedload sediment transport on the morphological evolution of the Medjerda should not be overlooked. Downstream of the confluence with the Oued Tessa, coarser sediments, sometimes up to 5 cm in diameter, have been observed up to 2 km downstream. Sandbanks have also been observed near

the Bousalem Bridge. This indicates that significant flood events can transport these bedload sediments. The percentage of sediment transport by bedload can reach 20 to 25% of the total sediment transport during exceptional flows (Gharbi, 2016). Therefore, we used these 5 classes of mean diameter for each scenario. Given the significant variation in particle diameters transported by bedload, we chose a diameter of 1 mm for sand particles (Table 1).

Table 1. Variation in sediment diameters based on water discharge

Q (m ³ /s)	% Clay (< 2 μm)	% Fine silt (2-20 μm)	% Coarse silt (20-50 μm)	Sand (> 50-2,000 μm)
100	25	32	29	14
200	26	28	27	19

2.6 Simulation scenarios and boundary conditions

The configuration of this section contains two distinct parts: the first part, located at the riverbed with a width less than 10 m, is entirely smooth with a roughness coefficient of 0.03 s/m^{1/3}. The second part, situated on both sides of the banks, exhibits variable roughness depending on the pre-existing vegetation cover. Four simulation scenarios were established, keeping the riverbed smooth and gradually increasing the roughness of the second part, with respective values of 0.03 s/m^{1/3}, 0.05 s/m^{1/3}, 0.07 s/m^{1/3}, and 0.09 s/m^{1/3}. These four scenarios are replicated for two constant discharge values of 100 m³/s and 200 m³/s, chosen as open boundaries at the model inlet. The output data is assigned to height data corresponding to the rating curve of the last section. Calibration results

from our previous studies in the analysis and mapping of floods in the Boussalem city will be taken into account.

2.7 Sediment transport analysis

The longitudinal profile analysis of the studied section of the Medjerda provides significant insights, highlighting a notable change in slope near the old bridge of Boussalem (Figure 5), where a slight increase from 0.24% to 0.36% is identified. Sandbars have also been observed near the Boussalem Bridge. Since the bed of the Medjerda, is mainly composed of silts and clays, the very low slopes of the riverbed do not allow for significant transport of coarser sediments by bedload.



Figure 5. Sediment deposits in the Medjerda River (downstream view of the old bridge of Boussalem)

The comparison between the 2007 and 2019 profiles reveals, upstream of the old bridge of Boussalem, moderate sedimentation with rates of 3.4 and 2.5 m³/mL/year (Figure 6). These rates, relatively low, take into account the dredging works carried out in the relevant sections, making it difficult to provide a precise quantitative estimation of the sedimentation process in this part. However, on the lower part, sedimentation increases significantly, reaching 9.5

m³/mL/year; this section corresponds to the entry of the influence zone of the dam on the longitudinal profile of the Medjerda. Given the limited changes in the longitudinal profile and the modest volumes transported by bedload, the observed changes in the sections are primarily attributable to variations (sedimentation/erosion) of fine particles within the sections.

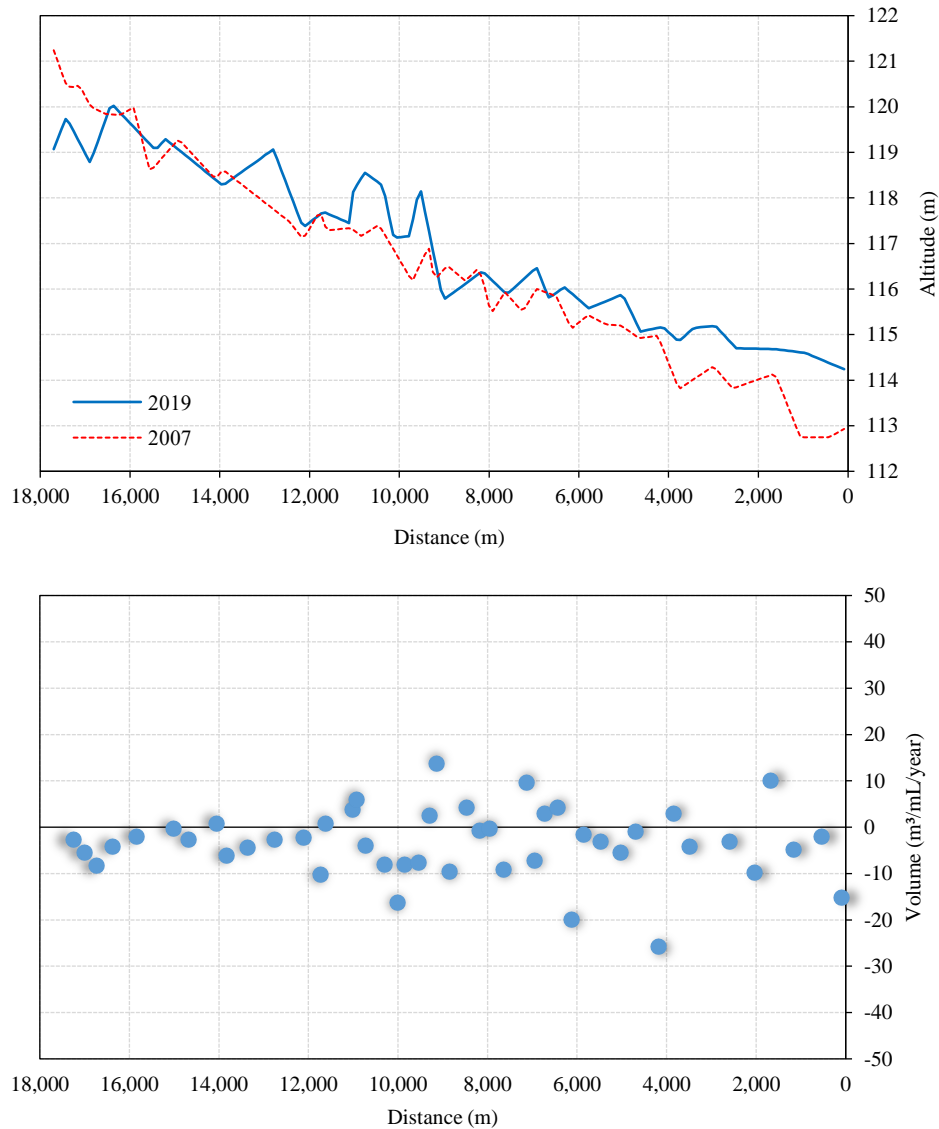


Figure 6. The riverbed evolution between 2007 and 2019 in the study area

3. RESULTS

The outputs generated by the model allowed us to conduct a comprehensive comparative analysis, focusing on flow velocity, shear stress, and bed evolution along the longitudinal profile and within each section. This helps in better understanding sedimentation patterns, predicting potential impacts on fluvial morphology, and aiding in the development

of sustainable water resource management strategies in the Medjerda Basin.

3.1 Velocity, shear stress, and bed evolution in a dredged riverbed

Figure 7 illustrates the velocity evolution along the longitudinal profile of the flow section in the first scenario, where the riverbed is considered completely

smooth. This scenario reflects the immediate reality on the ground after the completion of dredging works. It can be observed that the velocity undergoes multiple fluctuations, resulting from various factors such as slope, flow section width, depth, and changes in flow direction. The velocity decreases by approximately 0.2 m/s on average between the two discharges along the longitudinal profile.

Figure 7 also presents the calculated shear stress values for both discharges and at each section. Shear stress, representing the force per unit area acting parallel to the flow direction, influences the movement or retention of sediments on the riverbed. Despite the observed fluctuations due to different factors

governing the flow, there is a clear increase in shear stress, with an average of 2.3 N/m² with the increase in discharge.

The bed Shear stress is directly related to sediment transport capacity. An increase in shear stress leads to an increase in sediment transport and deposition, as clearly illustrated in Figure 8 where the longitudinal bed evolution is compared for the two discharges. It is observed that this evolution is more pronounced with the increase in discharge, reaching an average difference of 20 cm. This increase is explained by the increased force, causing erosion of the banks. The particles thus eroded subsequently undergo sedimentation in the flow bed.

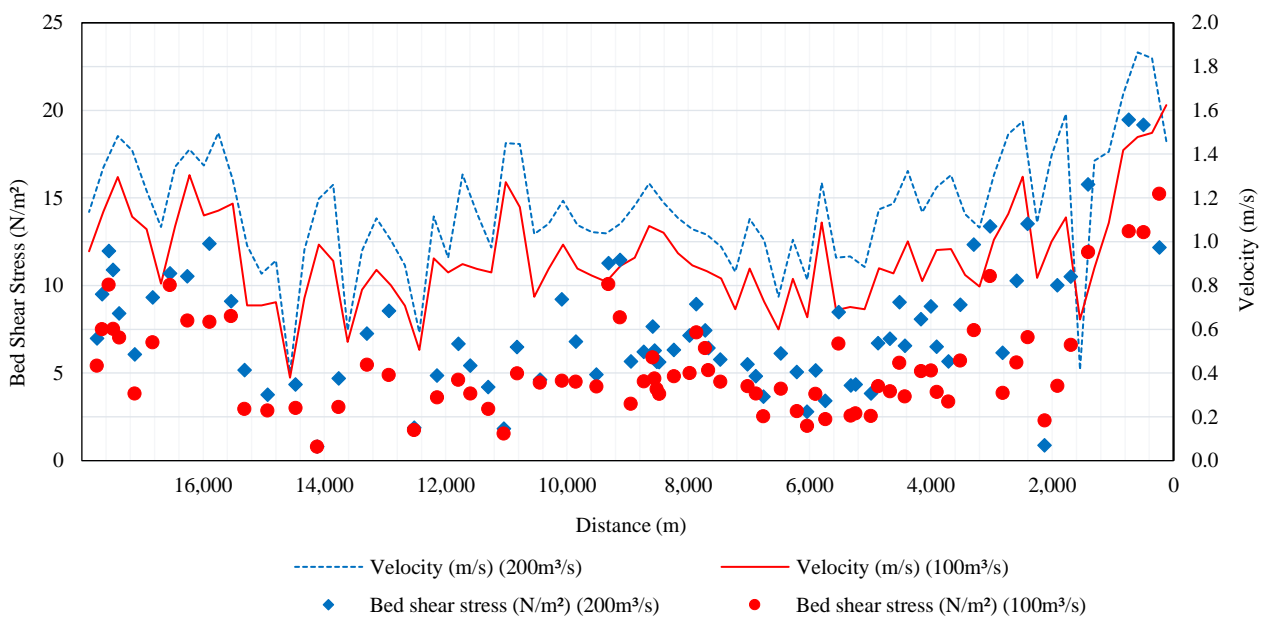


Figure 7. Velocity and longitudinal shear stress in a dredged riverbed for Q=100 m³/s and Q=200 m³/s

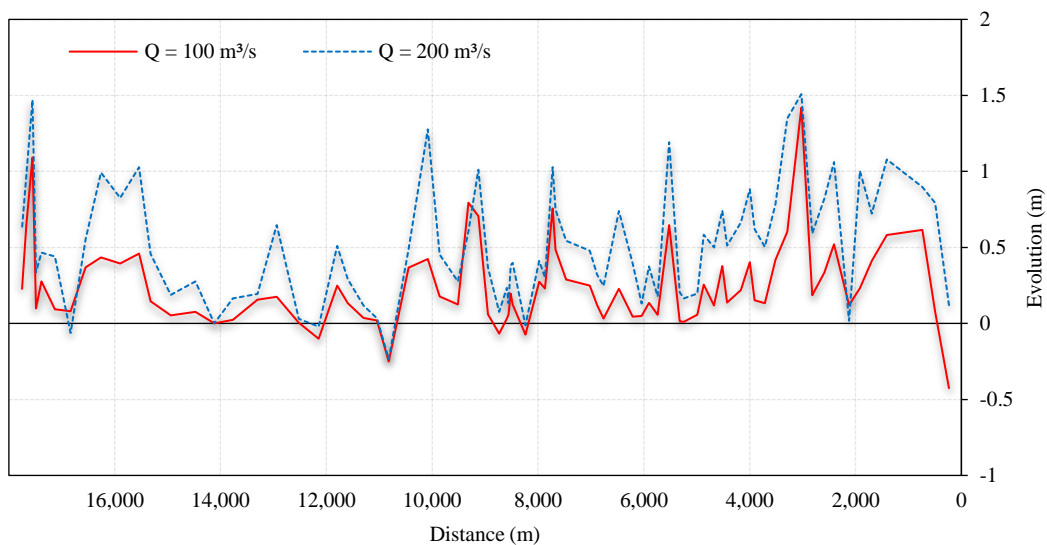


Figure 8. Longitudinal bed evolution in a dredged riverbed for Q=100 m³/s and Q=200 m³/s

3.2 Effect of roughness variation on velocity, shear stress, and bed evolution in transverse sections

Roughness increases in tandem with vegetation development. To assess the influence of vegetation on particle transport, we kept the riverbed smooth and gradually increased the roughness on both banks. Values of 0.03 s/m^{1/3}, 0.05 s/m^{1/3}, 0.07 s/m^{1/3}, and 0.09 s/m^{1/3} were respectively assigned to the vegetated area (Figure 9).

A cross-sectional analysis of the three parameters, namely velocity, shear stress, and bed evolution, was conducted for the four scenarios. As for the velocity (Figure 10), it exhibits a parabolic increase, reaching zero at the ends of both banks and attaining its maximum value in the middle of the section for the maximum water height. On the banks, we observe that the speed decreases as the roughness increases.

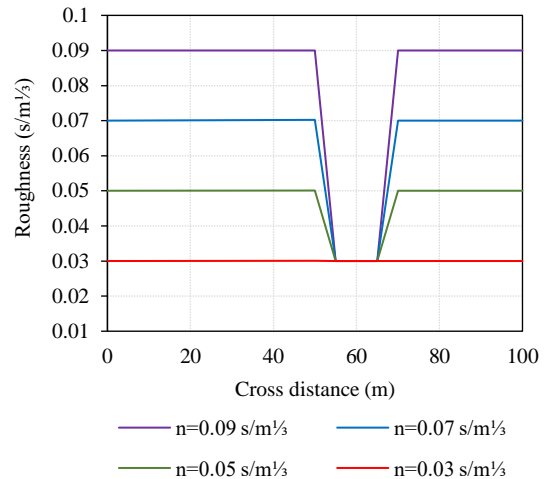
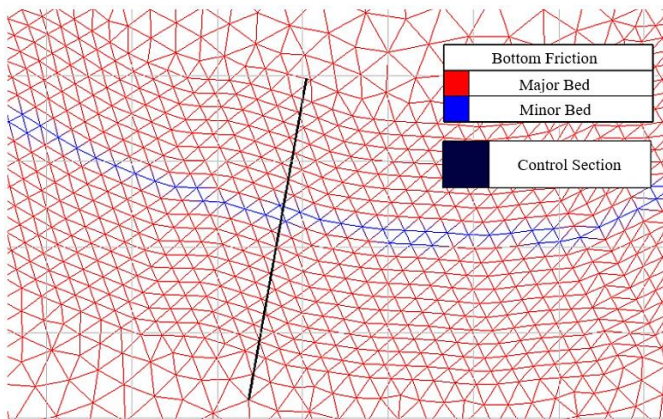


Figure 9. Variation of bed roughness in a cross-section

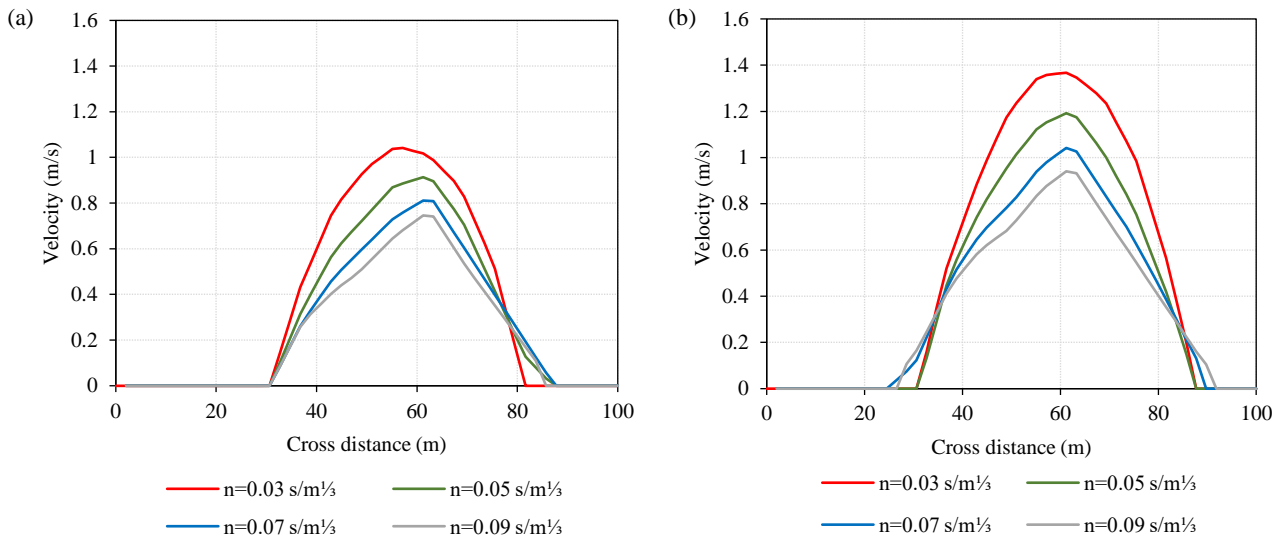


Figure 10. The average velocity Evolution in a cross-section as a function of roughness change for Q=100 m³/s (a) and Q=200 m³/s (b)

Furthermore, the evolution of the bed reveals the presence of two distinct regions. A deposition zone is observed on the smooth bed, while an erosion zone is noted along both banks, with a proportional decrease as roughness increases. For instance, under a discharge condition of 200 m³/s, erosion decreases from 50 cm in the first scenario to 8 cm in the second

scenario, almost disappearing in the last two scenarios. Meanwhile, the calculated maximum deposits are 80 cm, 41 cm, 28 cm, and 17 cm respectively for the four scenarios. This trend naturally stems from the reduction in the quantity of sediment transported by the water (Figure 11).

For the shear stress (Figure 12), it is observed that it increases as the roughness increases along the banks of the wadi. For a flow rate of 100 m³/s, the respective values are 6.1, 8.2, 10.2, and 12 N/m² for the four scenarios. In the middle part of the flow where the bed remains smooth, it is observed that the shear stress decreases for the four scenarios, with respective values of 6, 4.2, 3.1, and 2.6 N/m².

Analyzing these results, it becomes clear that vegetation plays a crucial role in preserving bank stability by acting as an effective barrier against particle detachment and suspension. This conclusion

is particularly reinforced by the observation in the last graph, where shear stress increases proportionally with the roughness coefficient on both banks. These findings suggest that the vegetation contributes to enhance the cohesion of the riverbed, minimizing the risks of erosion and excessive sediment transport (Figures 11 and 12). The combined effect of vegetation-induced roughness appears to play a crucial role in preserving bank stability, which can have significant implications for the management and preservation of river ecosystems

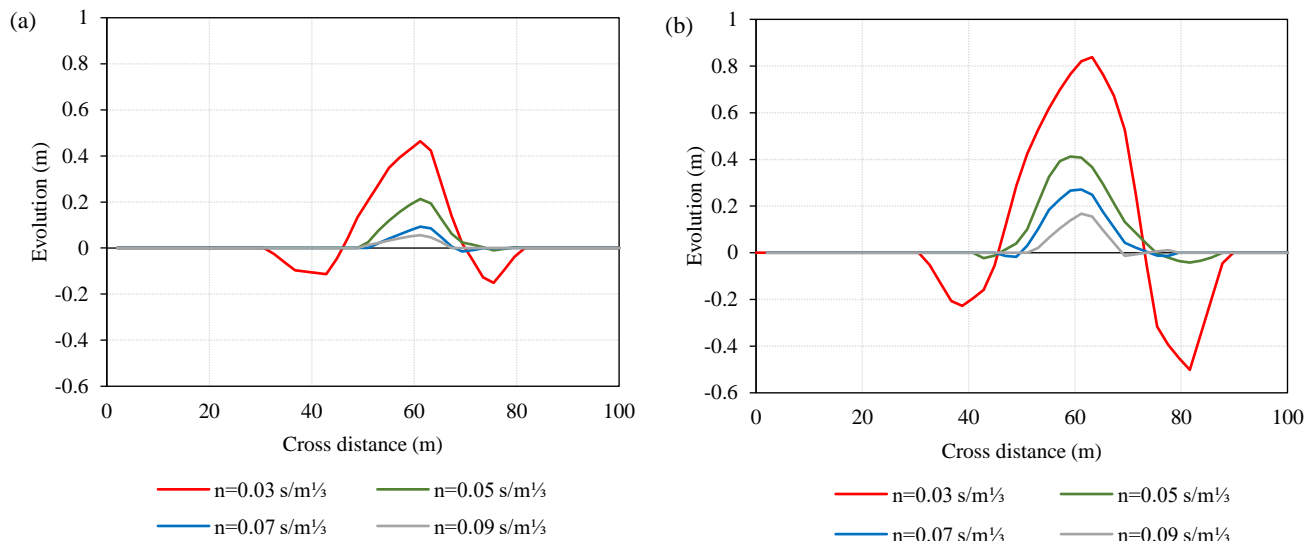


Figure 11. Bed evolution in a cross-section as a function of roughness change for Q=100 m³/s (a) and Q=200 m³/s (b)

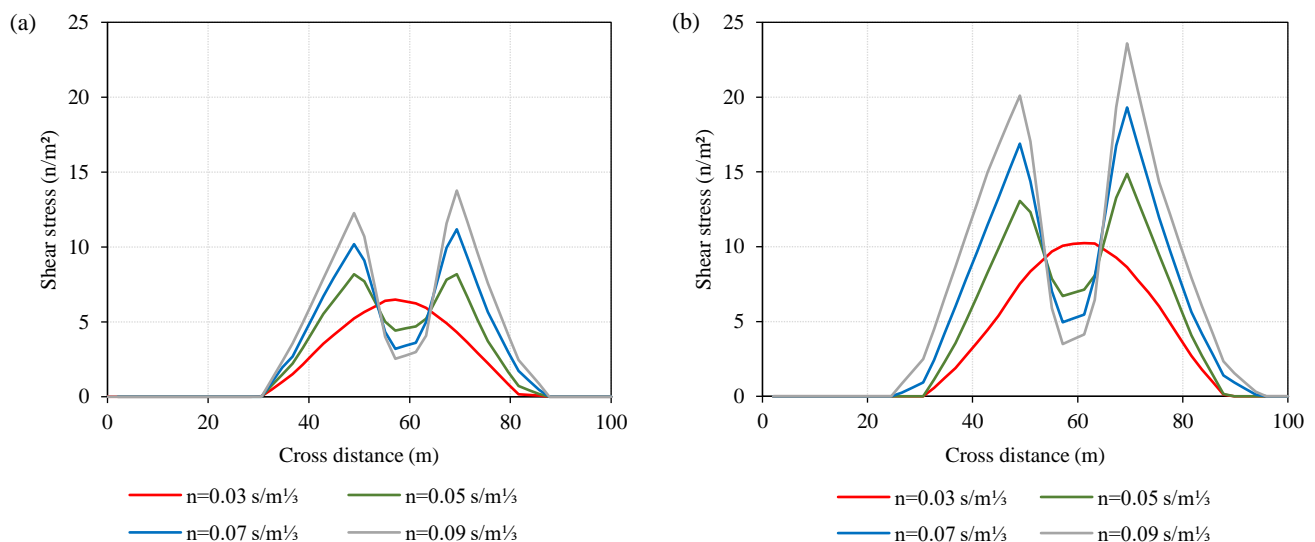


Figure 12. Bed shear stress evolution in a cross-section as a function of roughness change for Q=100 m³/s (a) and Q=200 m³/s (b)

3.3 Effect of roughness variation on the longitudinal evolution of the bed

The Figures 13 and 14 present a detailed analysis of the longitudinal evolution of the riverbed in response

to variations in bank roughness under different scenarios and for the two distinct imposed flow rates. For a flow rate of 100 m³/s, the maximum deposition decreases to values of 141 cm, 60 cm, 15 cm, and 8 cm,

respectively, while the maximum erosion decreases to values of 28 cm, 25 cm, 22 cm, and 11 cm. For a flow rate of 200 m³/s, the maximum deposition decreases to values of 150 cm, 72 cm, 42 cm, and 23 cm, respectively, and the maximum erosion decreases to values of 31 cm, 28 cm, 25 cm, and 22 cm, respectively. The observation of the data reveals a significant relationship between bank roughness and erosion and deposition phenomena in the riverbed.

When bank roughness increases, a noticeable trend emerges: the magnitude of erosion and deposition processes decreases. This observation suggests a substantial effect of the bank roughness on the sedimentary dynamics of the watercourse. It is essential

to notice that this trend is observed while keeping hydraulic parameters constant for the different scenarios studied, confirming the specificity of the effect of the bank roughness on the sediment transport.

The reduction in the magnitude of erosion and deposition phenomena indicates a relative stabilization of the riverbed as the bank roughness increases. This stabilization can be attributed to a decrease in the local flow velocity and an increase in shear stresses along the riverbed, resulting from increased roughness. These changes in hydraulic dynamics influence the river's ability to transport and deposit sediments.

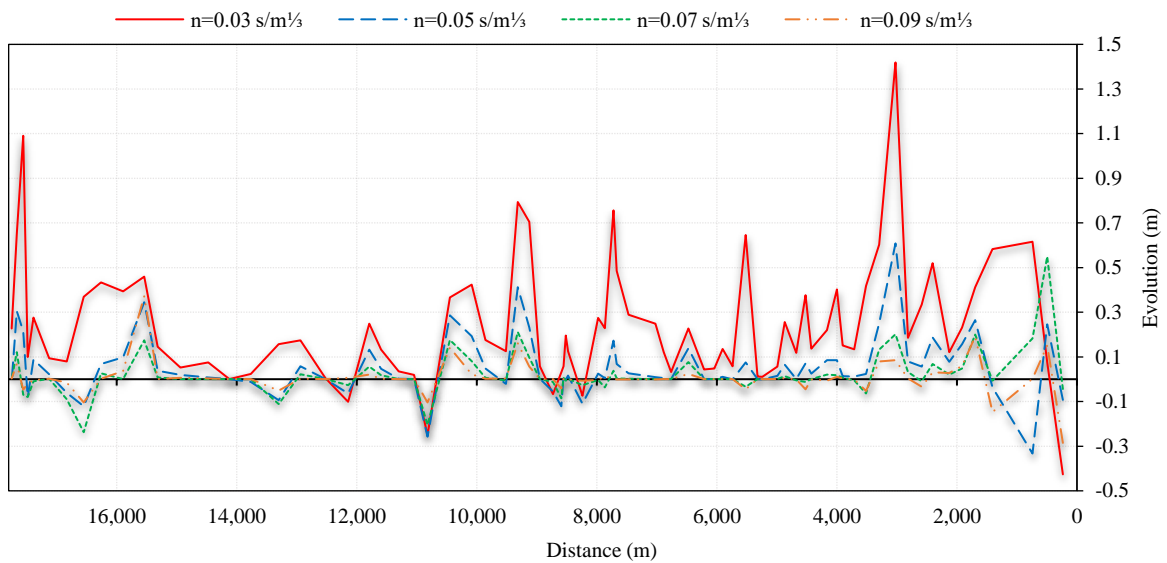


Figure 13. Evolution of longitudinal bed level in relation to variations in roughness for Q=100 m³/s.

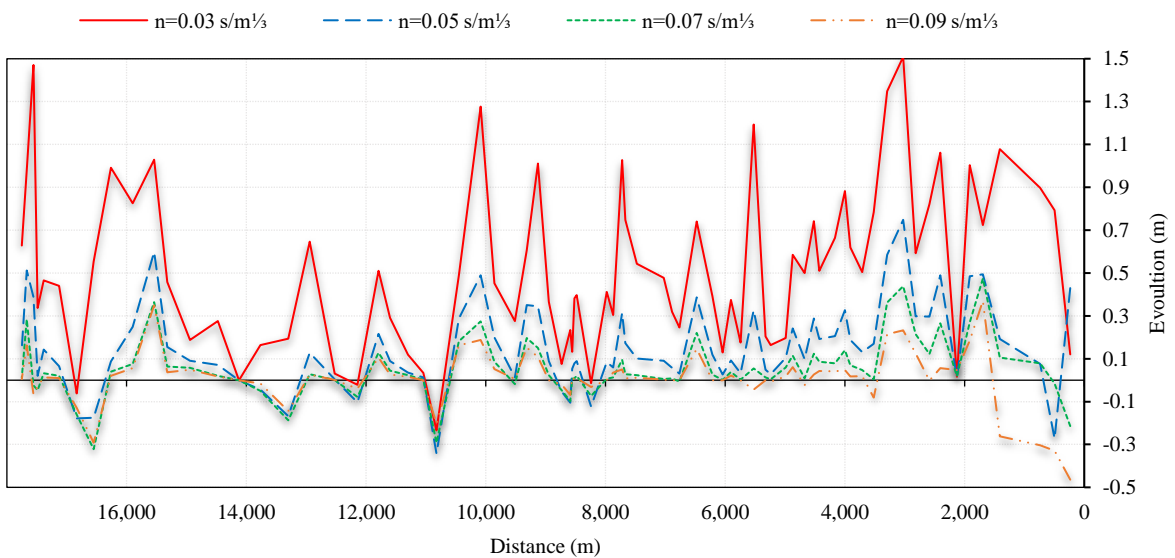


Figure 14. The longitudinal bed level evolution in relation to variations in roughness for Q=200 m³/s.

4. DISCUSSION

To better understand the impact of relative roughness on the morphology of the Oued, we calculated the following in the table: the average bed elevation (ζ_{mb}), the average bed shear stress (τ_{mb}), and the corresponding bed flow velocity (U_{mb}) for each scenario and for both discharge rates.

As relative roughness (λ) increases, the average bed shear stress (τ_{mb}) significantly decreases for a

discharge of 100 m³/s, dropping from 5.34 N/m² to 4.89 N/m², which is a reduction of approximately 8.4%. Similarly, for a discharge of 200 m³/s, τ_{mb} decreases from 7.46 N/m² to 6.52 N/m², representing a reduction of 12.6% with the increase in relative roughness (Table 2). This trend indicates that increasing relative roughness reduces the stress exerted by the flow on the smooth riverbed.

Table 2. Impact of relative roughness on bed elevation, shear stress, and flow velocity

	Q= 100 m ³ /s				Q= 200 m ³ /s			
	ζ_{mb} [m]	τ_{mb} [Nm ⁻²]	U_{mb} [ms ⁻¹]	q_b^* [m ³ s ⁻¹] (E-05)	ζ_{mb} [m]	τ_{mb} [Nm ⁻²]	U_{mb} [ms ⁻¹]	q_b^* [m ³ s ⁻¹] (E-05)
$\lambda_1=1$	0.241	5.34	0.93	1.72	0.431	7.46	1.15	3.32
$\lambda_2=2.15$	0.053	5.28	0.84	0.92	0.150	7.08	1.02	2.02
$\lambda_3=3.56$	0.018	5.05	0.74	0.36	0.054	6.83	0.94	1.49
$\lambda_4=5.19$	0.007	4.89	0.68	0.20	0.010	6.52	0.88	0.98

The average bed elevation (ζ_{mb}) decreases markedly with increasing relative roughness (λ). For a discharge of 100 m³/s, ζ_{mb} drops from 0.241 m to 0.007 m. Similarly, for a discharge of 200 m³/s, ζ_{mb} decreases from 0.431 m to 0.010 m. Given that the flow depth is around 3.32 m, the increase in relative roughness λ represents a depth increase of 7% and 12% respectively for the 100 m³/s and 200 m³/s flows (Table 2).

The bedload discharge significantly decreases with increasing relative roughness. For a discharge of 100 m³/s, q_b^* decreases from 1.72×10^{-5} m³/s to 0.20×10^{-5} m³/s as λ increases, representing a reduction of about 88%. Similarly, for a discharge of 200 m³/s, q_b^* decreases from 3.32×10^{-5} m³/s to 0.98×10^{-5} m³/s, which is a reduction of approximately 70% (Table 2). This marked decrease in bedload discharge with increasing relative roughness indicates the significant role of vegetated banks in reducing transported sediment. Our analyses suggest that dredging, although often used to increase flow discharge during flood events, could compromise bank stability by disrupting the natural sediment transport balance, potentially having adverse effects on the morphology of the Oued and on downstream reservoirs

Our results reflect the trends observed by Fan et al. (2023) regarding the increase in depth with increasing relative roughness. However, a direct comparison is challenging due to the variability in river dimensions on one hand, and the use of different particle diameter classes on the other. Despite these

differences, our results confirm the validity of previous observations in a slightly modified context.

Although our model simulates static roughness for different scenarios, the results obtained can serve as a foundation for initiating a dynamic roughness model. If we have real-time data on vegetation variability, this model would allow us to analyze the corresponding morphodynamic effects. For example, Fortes et al. (2022), through a dynamic model, demonstrated that the water level profile increased by an average of 7.03% over a one-year period, thereby highlighting the seasonal effect of vegetation

5. CONCLUSIONS

The objective of this study was to demonstrate how changes in bed roughness influence the morphodynamic evolution of the bed in response to sediment displacement. The study employed hydro-sedimentary numerical modeling using the hydrodynamic (TELEMAC 2D) and morphodynamic (SISYPHE) modules of the TELEMAC-MASCARET modeling system.

To highlight the effect of vegetation installed on the riverbanks on sediment transport and morphological deformation, we simulated scenarios with fixed roughness for the smooth bed and variable roughness for the banks, ranging from the smoothest to the roughest. Four simulation scenarios were established, progressively increasing the bank roughness with respective values of 0.03 s/m^{1/3}, 0.05 s/m^{1/3}, 0.07 s/m^{1/3}, and 0.09 s/m^{1/3}.

We analyzed the results on a control transverse section, as well as along the profile of the river. This analysis mainly focused on parameters of velocity, evolution, and shear stress. The results reveal two distinct zones in the evolution of the riverbed: a deposition zone on the smooth bed and an erosion zone along the banks. Erosion along the banks decreases proportionally with increasing roughness. This trend naturally results from the decrease in shear stress, which leads to a reduction in the amount of sediment transported by the water.

To assess the impact of the non-uniform distribution of bed roughness on the river's morphology, we used Einstein's method, which suggested using hydraulic radius segmentation to partition boundary resistance. For each relative bank roughness (λ), we calculated the average bed elevation (ζ_{mb}), the average bed shear stress (τ_{mb}), the flow velocity at the bed (U_{mb}), and the bedload discharge (q_b^*) for each scenario.

The results showed that the average bed elevation (ζ_{mb}) decreases significantly with increasing relative roughness (λ). Given that the flow depth is around 3.32 m, increasing the relative roughness λ from 1 to 5.19 results in an increase in depth of 7% and 12% respectively for flow rates of 100 and 200 m³/s. Our results reflect previously observed laboratory trends regarding the increase in depth with increasing relative roughness. However, direct comparison is challenging due to variability in river dimensions and the use of different particle diameter classes. Despite these differences, our results confirm the validity of previous observations in a slightly modified context.

The results also show that:

- With increasing relative roughness (λ), the average shear stress (τ_{mb}) decreases significantly by about 8.4% and 12.6% respectively for flow rates of 100 and 200 m³/s.
- The bedload discharge (q_b^*) decreases significantly with reductions of approximately 88% and 70% respectively for flow rates of 100 and 200 m³/s.

Although dredging works combat flooding by facilitating flow transit, they lead to increased amounts of transported sediments that will deposit downstream in the dams due to the removal of vegetation, which is crucial for the morphological stability of the river. This reduces the exploitable water volume in the dams and accelerates its silting. The results obtained can serve as a foundational basis for initiating a dynamic

roughness model if real-time roughness variability data is available.

REFERENCES

- Badoux A, Andres N, Turowski JM. Damage costs due to bedload transport processes in Switzerland. *Natural Hazards and Earth System Sciences* 2014;14(2):279-94.
- Exner FM. On the Physics of Dunes. Vienna, Austria: Proceedings of the Academy of Sciences in Vienna; 1920 (in German).
- Einstein HA. Formula for transportation of bed load. *Transactions of the American Society of Civil Engineers* 1942;107(1): 561-97.
- Einstein HA. The bed load function for sediment transportation in open channel flows. In: *Technical Bulletin*. USA: U.S. Department of Agriculture; 1950. p. 71.
- Fan J, Huang H, Yu G, Su T. River channel forms in relation to bank steepness: A theoretical investigation using a variational analytical method. *Water* 2020;12(5):Article No. 1250.
- Fan J, Luo Q, Bai Y, Liu X, Li R. Investigating the influence of the relative roughness of the riverbanks to the riverbed on equilibrium channel geometry in Alluvial Rivers: A variational approach. *Water* 2023;15:Article No. 4029.
- Fortes AA, Hashimoto M, Udo K, Ichikawa K, Sato S. Dynamic roughness modeling of seasonal vegetation effect: Case study of the Nanakita River. *Water* 2022;14:Article No. 3649.
- Gharbi M, Soualmia A, Dartus D, Masbernat L. Floods effects on rivers morphological changes: Application to the Medjerda River in Tunisia. *Journal of Hydrology and Hydromechanics* 2016;64(1):56-66.
- Gharbi M. Study of Floods and Associated Sediment Transport - Application to the Medjerda Watershed [dissertation]. Toulouse: National Polytechnic Institute of Toulouse; 2016.
- Guan M, Carrivick JL, Wright NG, Sleigh PA, Staines KE. Quantifying the combined effects of multiple extreme floods on river channel geometry and on flood hazards. *Journal of Hydrology* 2016;538:256-68.
- Hammami S, Romdhane H, Soualmia A, Kourta A. 1D/2D coupling model to assess the impact of dredging works on the Medjerda River Floods, Tunisia. *Journal of Materiel and Environmental Science* 2022;13(7):825-39.
- Hammami S, Soualmia A, Kourta A. Analysis and forecasting flood risk mapping of the Medjerda River at Boussalem Town, in Tunisia. *Engineering and Applied Science Research* 2023;50(5):449-57.
- Hammami S, Soualmia A, Kourta A. Telemac 2D modeling of pollutant transport in the Medjerda River: Impact of Tamarix Vegetation, Bousselem, Tunisia. *European Journal of Environment and Earth Sciences* 2024;5(3):47-54.
- Hervouet J-M. *Hydrodynamics of Free Surface Flows: Numerical Modeling with the Finite Element Method*. Paris, France: Presses de l'École Nationale des Ponts et Chaussées; 2003.
- Li J, Claude N, Tassi P, Cordier F, Vargas-Luna A, Crosato A, et al. Effects of vegetation patch patterns on channel morphology: A numerical study. *Journal of Geophysical Research: Earth Surface* 2022;127(5):e2021JF006529.
- Luca M, Diego R, Walter B. The role of vegetation and large wood on the topographic characteristics of braided river systems. *Geomorphology* 2020;367:Article No. 107299.
- Meyer-Peter E, Müller R. Formulas for bed-load transport. *Proceedings of the 2nd Meeting of the International*

- Association for Hydraulic Structures Research; 1948 May 7; Stockholm; 1948.
- Morri M, Soualmia A, Belleudy P. Mean velocity predictions in vegetated flows. *Journal of Applied Fluid Mechanics* 2016;9(3):1273-83.
- Mugade U, Sapkale J. Influence of aggradation and degradation on river channels: A review. *International Journal of Engineering and Technical Research* 2015;3(6):209-12.
- Nanson RA, Nanson GC, Huang HQ. The hydraulic geometry of narrow and deep channels: Evidence for flow optimization and controlled peatland growth. *Geomorphology* 2010;117(1-2):143-54.
- Nazarjani M, Saremi A, Eslami AR, Yazdani V. Analysis of the impact of roughness coefficient changes due to land use changes on the hydraulics of the Kashafrood River. *AQUA - Water Infrastructure, Ecosystems and Society* 2023; 72(11):1969-86.
- Nazi MHM, Awang S, Shaaban AJ, Yahaya NKEM, Jusoh AM, Arumugam MARMA, et al. Sediment transport dynamic in a meandering fluvial system: Case study of Chini River. *IOP Conference Series: Materials Science and Engineering* 2016;136:Article No. 012072.
- Penna N, Coscarella F, D'Ippolito A, Gaudio R. Effects of fluvial instability on the bed morphology in vegetated channels. *Environmental Fluid Mechanics* 2022;22(2):619-44.
- Ramirez JA, Zischg AP, Schürmann S, Zimmermann M, Weingartner R, Coulthard T, et al. Modeling the geomorphic response to early river engineering works using CAESAR-Lisflood. *Anthropocene* 2020;32:Article No. 100266.
- Recking A. An analysis of nonlinearity effects on bedload transport prediction. *Journal of Geophysical Research* 2013;118:1264-81.
- Reisenbüchler M, Bui MD, Skublics D, Rutschmann P. Enhancement of a numerical model system for reliably predicting morphological development in the Saalach River. *International Journal of River Basin Management* 2019;18(3):335-47.
- Rickenmann D, Badoux A, Hunzinger L. Significance of sediment transport processes during piedmont floods: the 2005 flood events in Switzerland. *Earth Surface Processes and Landforms* 2016;41(2):224-30.
- Tu T, Carr KJ, Ercan A, Trinh T, Kavvas ML, Nosacka J. Assessment of the effects of multiple extreme floods on flow and transport processes under competing flood protection and environmental management strategies. *Science of the Total Environment* 2017;607-608:613-22.
- Van Rijn LC. Sediment transport, Part I: Bed load transport. *Journal of Hydraulic Engineering* 1984;110(10):1431-56.
- Vargas-Luna A, Crosato A, Byishimo P, Uijtewaal WSJ. Impact of flow variability and sediment characteristics on channel width evolution in laboratory streams. *Journal of Hydraulic Research* 2019;57(1):51-61.
- Wilcock PR, Crowe JC. Surface-based transport model for mixed-size sediment. *Journal of Hydraulic Engineering* 2003; 129(2):120-8.
- Yassine R, Cassan L, Roux H, Frysou O, Pérès F. Numerical modelling of the evolution of a river reach with a complex morphology to help define future sustainable restoration decisions. *Earth Surface Dynamics* 2023;11(6):1199-221.